

A Simple Process for Fabricating Organic/TiO₂ Super-Hydrophobic and Anti-Corrosion Coating

Chunyan Mo¹, Yansheng Zheng^{1,2,*}, Falong Wang¹, Qian Mo¹

¹ College of Biological and Chemical Engineering, Guangxi University of Science and Technology, Liuzhou 545006, Guangxi, PR China

² Lushan College of Guangxi University of Science and Technology, Liuzhou 545616, Guangxi, PR China

*E-mail: 2320989563@qq.com

Received: 2 June 2015 / Accepted: 9 July 2015 / Published: 28 July 2015

Fluoro-methylhydro-silicone oil was blended with nano TiO₂ particle after it was prepared by methylhydro-silicone oil and dodecafluoroheptyl-propyl-trimethoxysilane as raw materials. The Organic/TiO₂ composite coating was fabricated on steel substrate by sol-gel method. The hydrophobicity and surface structure of composite coating were described by Infrared spectroscopy, Scanning electron microscopy, thermogravimetric analysis and Contact angle analyzer. In addition, Electrochemical methods were measured in order to characterize the corrosion of the as-prepared coating. The results indicated that the final composite coating with rich surface structure had a good anti-corrosion performance and exhibited superhydrophobic.

Keywords: Organic/TiO₂ composite coating; super-hydrophobic; anti-corrosion

1. INTRODUCTION

The wettability of solid surface, which governed by not only the morphology of the solid surface but also its intrinsic chemical compositions, is one of the most important properties of solid surface[1,2]. It's characterized by contact angle and sliding angle. We call the solid surface as super-hydrophobic surface when its contact angle (CA) is larger than 150° while sliding angle (SA) is smaller than 10°[3-5]. These special surface can be commonly found in biological system such as animal bodies and plants. for example, the lotus leaf is a typical model with both super-hydrophobicity and low adhesive force, whereas[6], the gecko is a typical model which represents the Cassie impregnating wetting state with super-hydrophobicity but high adhesive force[7,8]. In recent years, Super-hydrophobic materials have gained a significant interest and are of interest for various fields such as

metal anti-corrosion[9], self-cleaning[10,11], building waterproof[12], fluid drag reduction[13] and anti-fouling[14] as well owing to their peculiar and improved features.

As we all know, numerous of coating techniques for fabricating super-hydrophobic surfaces have been reported, including chemical vapor deposition, phase separation, sol-gel process, electro-spinning and etching (plasma etching, photo etching, acid etching) method[15-18]. The principle of all the methods mentioned above in fabricating super-hydrophobic surfaces is widely accepted as either creating the rough structure on the surface of hydrophobic materials directly or modifying a rough surface by materials with low surface free energy, or combining both[19-21]. Some materials such as glass, wood, cotton cloth, paper, plastics and metals are used as substrates to create artificial superhydrophobic surfaces[22-24]. In the meantime, a large number of chemical substances including Silane[25], Fluoroalkylsilane[26] and Teflon[15] are used to modify the surface with micro/nanometer scale during the modification process. Thanks to the special apparatus for limited base materials, rigorous conditions and multi-step, the cost of most techniques seems to be unacceptable and the time consuming seems to be impractical [27]. How to develop preparation process, especially easy-to-prepare, high-efficiency, low-cost and large-scale, plays a key role in fabricating super-hydrophobic surfaces. And, for now at least, much effort has been put toward expanding applications of artificial superhydrophobic surfaces[28].

In the few past decades, composite material has attracted considerable attention within fundamental research as well as potential application industry because of its special advantages[26]. In addition, it had an incredible tremendous progress in such a short period of time because of the huge demand for more functional and advanced materials. Compared with the properties of a single material, composite materials have more advantages including higher thermal stability, better dimensions, better mechanical behavior[29,30]. For instance, as a new composite between organic polymer and inorganic polymer, the organic-inorganic nano-meter composite material can overcome the disadvantages of single organic or inorganic nano-particle in order to satisfy utilization requirements. For now, the composite material have concurrently characteristic of inorganic-organic matter. What's more, the organic-inorganic nano-meter composite material with special functions has been widely used in many applications. Throughout this process, nano-meter inorganic powders are usually used as filling materials to be combined with organics by chemical bound in order to endued the product with excellent properties such as super-hydrophobic performance because of its micro/nano secondary structure. As super-hydrophilic substance, the nano-particles of titanium dioxide has a large number of hydroxyl groups on its surface, they are easily agglomerated in the water emulsion due to the high surface energy, in fact, the modification of nano-titanium dioxide powder is necessary so that the super-hydrophobic coating can be obtained. Silane coupling agent and fatty acids are the common modifiers. Hu et al.[31] fabricated the nano-titanium dioxide (nano-TiO₂) super-hydrophobic surface on Hastelloy substrate after suitable thermal treatment through simple dip-coating. The nano-TiO₂ solution was used as precursor solution and fluorinealkylsiloxane was used as modifier, the results showed the as-obtained sample had excellent superhydrophobicity with water contact angle higher than 170°. Ramanathan [32] Fabricated superhydrophobic surfaces in aqueous(ethanol/water) or non-aqueous(xylene) solvent via a very simple and inexpensive method by using titanium dioxide and trimethoxypropyl silane as raw materials. The results showed the surfaces

formed in different solvents had same static contact angle as high as 160° but different adhesion and contact angle hysteresis. Based on a convenient and controllable strategy, Wang et al.[33] prepared a superhydrophobic TiO_2 film on glass substrate followed by thermal treatment and modification with stearic acid, the as-prepared film exhibited improved transparency, good bounce performance and high superhydrophobicity, the water contact angle as high as 157° , in contract, the low roll-off angle was 2° . In this letter, we developed a simple method for fabricating superhydrophobic and anti-corrosive composite coating by nano modified TiO_2 and Fluoro-methylhydro-silicone oil. the CA is up to $151.5^\circ \pm 1^\circ$ and SA is down to 6° . The morphological and wetting properties of the coating surfaces are investigated as well as the anticorrosion performance of the composite coating. The results show the composite had rough surface with rich structure and good anticorrosion performance.

2. EXPERIMENTAL DETAILS

2.1 Materials

TiO_2 with average particle size 10-30 nm was purchased from Shanghai jiang titanium dioxide chemical products co., LTD. Methylhydro-silicone oil with hydroxylgroup content between 6 and 10 was obtained from Jinan heng Feilong chemical co., LTD. Stearic acid was obtained from Guangdong Shantou Xilong chemical plant. Dodecafluoroheptyl-propyl-trimethoxysilane (DFPT) was obtained from Haerbing Xeogia fluoro-silicone Chemical Reagent Co.,Ltd. Sodium Dodecyl Benzene Sulfonate (SDBS) was obtained from Shantou guanghua chemical plant. ammonia solution ($\text{NH}_3 \cdot \text{H}_2\text{O}$) and ethanol were analytical grade and used as received.

2.2 Modification of nano TiO_2 particles

First of all, orderly add TiO_2 (5g) and stearic acid (0.4 g) that was well dissolved in ethanol (40 mL) into 40 mL of DI water under magnetic stirring for more than 2h at 80°C followed by adding suitable SDBS. The pH of TiO_2 hybrid emulsion was adjusted to 5.0 by the addition of acetic acid. Finally, the modified-nano TiO_2 was dried at the tempature of 130°C for 2 h.

2.3 Fabrication of fluoro-methylhydro-silicone oil

The fluoro-methylhydro-silicone oil was prepared by dehydrogenation coupling reaction. First, Mix SDBS (0.1 g) and DI water (20 mL) with a low speed for 5 min at room temperature. Then, slowly add Dodecafluoroheptyl-propyl-trimethoxysilane: methylhydro-silicone oil (1:1), ethanol (10 mL) and suitable catalyst Karstedt into the solution above. The mixture was called solution A and it was vigorously stirred for another 3 h until the reaction was complete.

2.4 Fabrication of superhydrophobic composite coating

The as-prepared modified TiO₂ powder was slowly added into solution A as well as silane coupling agent (3-(Methylacryloxy) propyltrimethoxy silane) and two drops of catalyst (ammonia solution). Followed, a homogeneous white viscous liquid was obtained after the mixture had been stirred for 4 h and aged at room temperature for 12 h. Based on the combined effect of the chemical bonding force among particles and the absorption force of substrate surface, the Organic/TiO₂ coatings were directly made on cleaned substrate after dip-coating and a series of heat-treatment process. Fig. 1 shows the schematic illustration of preparing superhydrophobic composite coating.

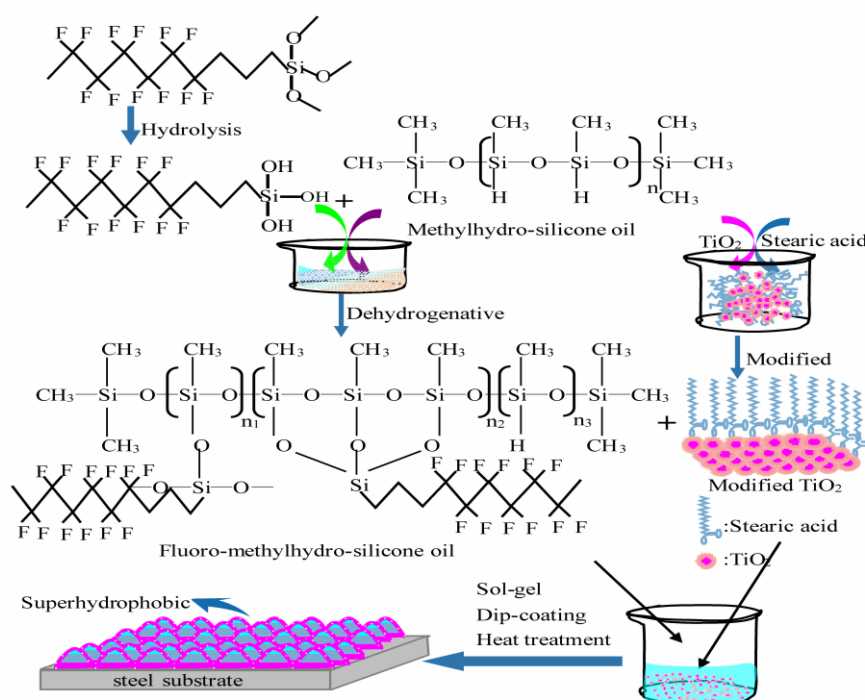


Figure 1. The process of forming the composite coating

2.5 Characterization

The final composite particle was tested with thermal analysis (TG, Netzsch STA449F3A-1103-M) and its surface morphology structure was characterized by digital scanning electron microscopy (SEM, S-3400 N), The water CA and SA of the composite coating surface were obtained by averaging the measurements on five positions of the examined surface through sessile drop method (Dataphysics OCA20), and the corrosion of the composite coating was characterized by electrochemical methods such as polarization measurement and alternating current impedance spectroscopy through CHI 660D electrochemical analyzer, Fourier transform infrared (FTIR) spectra were recorded with a Nicolet 380 spectrometer in the range 4000-500 cm⁻¹.

3. RESULTS AND DISCUSSION

3.1 FT-IR spectra

Fig. 2 shows the FTIR spectras of original and fluorinated methylhydro-silicone oil with DFPT. In the low frequency region, the Si-O-Si group and -CH₂- group stretching vibration peaks appear at around 800 cm⁻¹ and 1100 cm⁻¹ in both methylhydro-silicone oil and fluoro-methylhydro-silicone oil spectra. The -OCH₃ group in DFPT will be hydrolyzed into hydroxyl radica(-OH) and then reacted with the Si-H group in methylhydro-silicone oil when the catalyst Karstedt exists[34], so the presence of the absorption band at 2167 cm⁻¹ in methylhydro-silicone oil spectra which is attributed to Si-H stretching vibration disappears after the reaction with DFPT. What's more, The two other absorption bands at 1710 cm⁻¹ and 2925 cm⁻¹ in fluoro-methylhydro-silicone oil are due to the stretching vibration of -CH₃ and CF₂-CF₂ groups[35]. The results further confirm that the methylhydro-silicone oil has been successfully fluorinated.

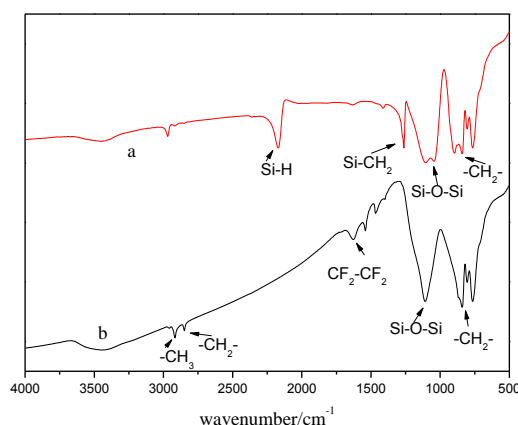


Figure 2. The infrared spectrograms of samples: (a) methylhydro-silicone oil; (b) fluoro-methylhydro-silicone oil

3.2 Thermal analysis

As we all know, heat treatment has an effective influence on surface chemical composition and the microstructure of composite particles[36]. Furthermore, both surface chemical composition and microstructure will determine the wettability of the composite coating[37,38]. Reacting process of the composite particles with temperature is understood through determining its thermal analysis curves. Fig. 3 shows the effect of heat treatment on the hydrophobicity of the TiO₂-fluoro-methylhydro-silicone oil composite coatings, The samples were heated at different temperatures including 60, 90, 120, 130, 150 and 180 °C for 1 h. We can see from Fig. 3 that the coating attained the best hydrophobic property (WCA = 151.5 ± 1°) when the temperature was 130 °C. Fig. 4 presents the TG-DSC curve of the as-prepared composite particles when the temperature was about 130 °C. According to the TG-DSC curve. The exothermic peak and weight loss at about 160 °C in the TG-DSC curve is

mainly due to the microscopic chemical reagents and physical absorbed water's desorption behaviours. In addition, The obvious exothermic phenomenon and mass-loss rate of composite particles achieves when the temperature is between 300 °C and 800 °C especially at about about 670 °C, which mean the composite particles are suffering from damage thermally during this period. This may because of the oxidative and decomposition of stearic acid, alkyl groups, organofluorine and other organic material.

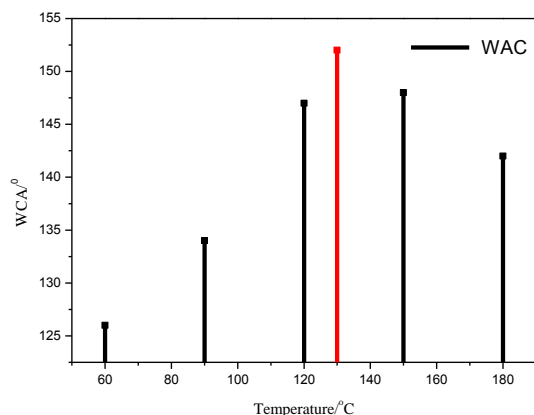


Figure 3. Effect of heat treatment on water contact angle

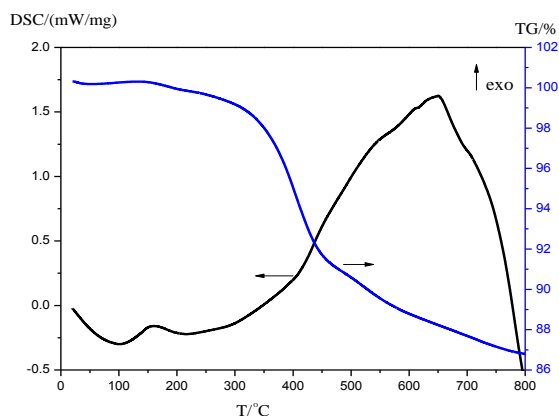


Figure 4. Thermal analysis curves of as-prepared composite particles

3.3 Morphological studies

Wettability of solid surface is governed by both the chemical composition and the surface microstructure roughness. Fig.5 shows the microstructures of the as-prepared samples in our case. The fluoro-methylhydro-silicone oil particles showed in Fig. 5a-b exhibit unique hierarchical soft air-cushion structures that can adsorb a large fraction of air. After reacted with nano-modified TiO₂, these soft air-cushion structures are full of inorganic powder so the morphology structures of composite particles are more abundant (Fig. 5c-d). According to the famous Cassie and Baxter module[39], instead of being full filled with liquid directly, there has a large quantity of air between the grooves on solid surface and the liquid. Such special gas-liquid-solid composite interface, which is

closely related to the micro/nano double structures on the hierarchically rough surface, is required for superhydrophobicity. This configuration is described by the following Eq. (1): $\cos\theta_{CB}=f\cos\theta+f-1$ [39-42]. Where θ_{CB} and θ respectively denote the contact angle of a water droplet on a rough surface and on a smooth surface, f is the liquid-solid surface fraction. It is easy to deduce from Eq. (1) that the more hydrophobic the composite coating appears as the CA of the rough surface (θ_{CB}) increase and the liquid-solid surface fraction (f) decrease. In our study, the images of the superhydrophobic properties of the uncoated and coated coatings are showed in Fig.6, showing the water contact angle of TiO_2 /fluoro-methylhydro-silicone oil composite coating reaches $151.5 \pm 1^\circ$.

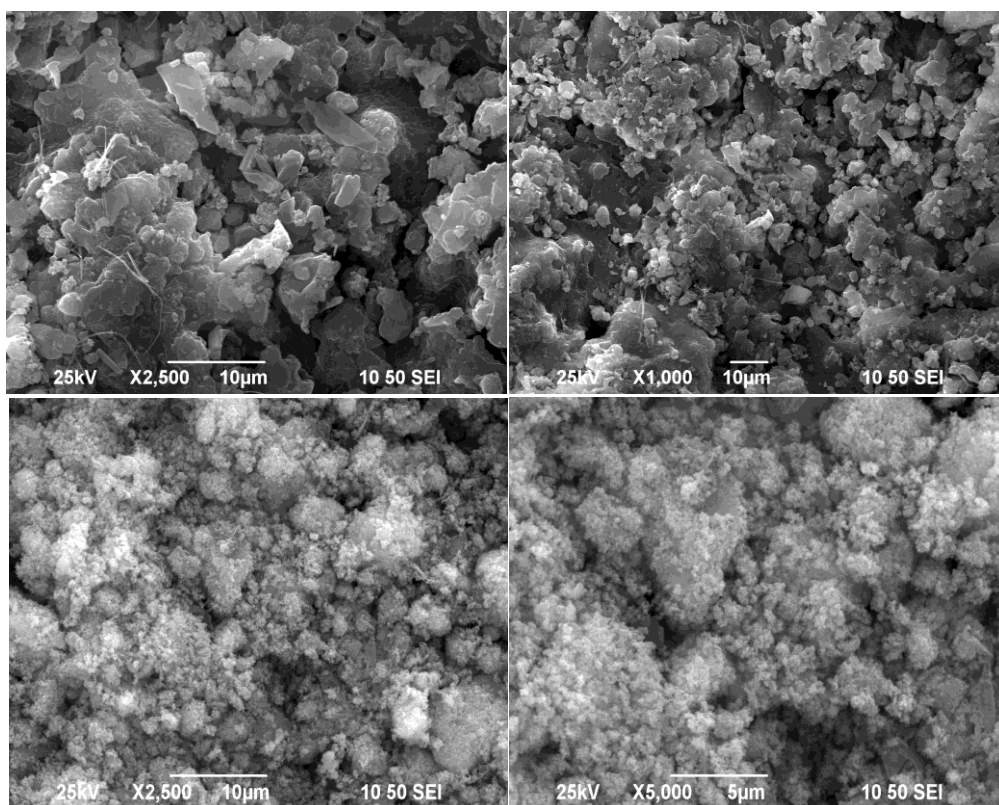


Figure 5. SEM images of the samples:(a-b) fluoro-methylhydro-silicone oil particles, (c-d) modified nano TiO_2 /fluoro-methylhydro-silicone oil composite particles

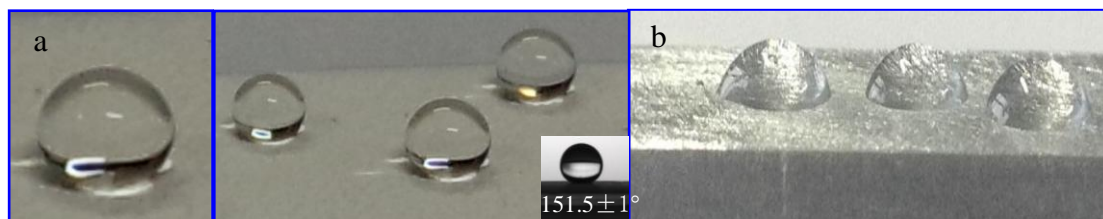


Figure 6. Images of the water droplets on the as-prepared coating surface: (a) TiO_2 /fluoride-methylhydro-silicone oil particles, (b) uncoated steel substrate

3.4 Electrochemical measurements

The anti-corrosion performance of five different samples were described based on a series of electrochemical measurements in order to further examine their corrosion behaviors. All samples were tested after being immersed in 3.5 wt% NaCl aqueous for 48 h under air-open condition with a three-electrode system at room temperature. The coating specimen was used as the working electrode. A saturated calomel electrode and a platinum electrode were used as reference electrode and auxiliary electrode, respectively.[19,43] The polarization measurements were conducted at a scanning rate of 5 mV/s, the potential range was from -1.4 to 0.6 V.

Fig. 7 shows the Tafel plots of uncoated/coated steel samples and the parameters obtained from potentiodynamic polarization measurements including corrosion potential (E_{corr}), corrosion current density (j_{corr}), anodic and cathodic Tafel constants (β_a and β_c) are given in Table 1. According to Fig. 7 and table 1, E_{corr} increased to -0.91 V, -0.98 V and -0.93 V from -1.15 V for bare steel after being coated with modified nano-TiO₂, methylhydro-silicone oil and fluoro-methylhydro-silicone oil, respectively. We can also observed that TiO₂/fluoro-methylhydro-silicone oil exhibited the most positive E_{corr} compared to the other samples. It's corrosion potential was -0.85 V. These positive shifted in E_{corr} confirms the protection of steel substrate surface when the composite was coated on. someone believed that the shifts in E_{corr} might due to the development of more stable passive films, similar to anodic protection.[44,45] In addition, the similar trend was observed in β_a and β_c . Compared with the bare steel substrate, the samples coated with modified nano-TiO₂, methylhydro-silicone oil and fluoro-methylhydro-silicone oil, respectively showed a rising trend in whole though with a minor fluctuation. This may account for the positive shifts in E_{corr} . Moreover, according to Table 1, the corrosion current density (j_{corr}) of TiO₂/fluoro-methylhydro-silicone oil was 3.44×10^{-5} A/cm², which was 223.26, 4.85, 4.56, 2.85 times lower than that of uncoated, TiO₂, methylhydro-silicone oil and fluoro-methylhydro-silicone oil films. The significant decrease in j_{corr} suggested that the organic/ TiO₂ composite coating was of good sealing type.[46]

The Nyquist plots of the measured samples are showed in Fig. 8, Where Z' (Z'') mean the real (imaginary) part of the impedances. The charge transfer resistance, which can be obtained from the diameter of the EIS curve, is used to evaluate whether the coating exhibit good anti-corrosion performance or not[42,47]. Generally, the slower corrosion rate is, the higher corrosion resistance is, the bigger charge transfer resistance with higher corresponding curve radius is, and vice verse. As easily unsterstood from Fig. 8, the diameter of the EIS curve of bare steel substrate was much smaller than other samples. The methylhydro-silicone oil showed similar anti-corrosion performance compared with pure modified TiO₂ coating but poorer than fluoro-methylhydro-silicone oil. what's more, the diameter of the EIS curve of TiO₂/fluoro-methylhydro-silicone oil was the highest one.

Based on the results above, we do believe that the TiO₂/Organic coating exhibited the best corrosion protection on steel substrate, which may due to the effective interactions between fluoro-methylhydro-silicone oil organic macromolecule and nano-TiO₂ inorganic powders. the presence of TiO₂ nanoparticles significantly improved a micro/nano double rough surface[48], which created a gas-liquid-solid composite interface, neither active chloride ions nor water molecules in NaCl solution that would promote corrosion to accelerate the damage to coating[49] can readily penetrate the

composite structure. What's more, the organic macromolecule fluoro-methylhydro-silicone oil with hydrophobic alkyl groups and a network of Si-O groups can decrease the effective area for corrosion reaction by blocking the reaction sites in order to prevent the substrate being corroded. The anti-corrosive mechanism of as-prepared Organic/TiO₂ composite coating is shown in Fig.9. However, both methylhydro-silicone oil and fluoro-methylhydro-silicone oil were somehow more sticky to water as well as the pure TiO₂ film, thus showed poorer anti-corrosion performance (higher j_{corr} and lower E_{corr}) than TiO₂/organic composite coating. Last but not least, the bare steel substrate was immersed in corrosive medium directly so it is unable to protect itself from being corroded.

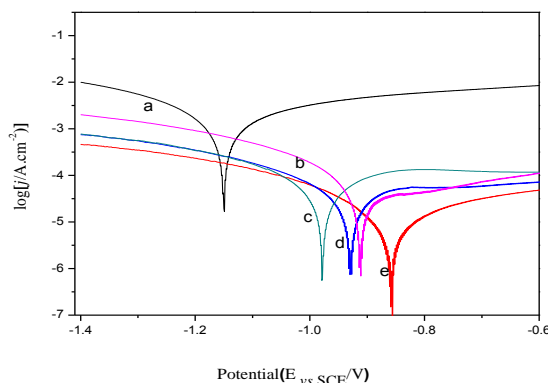


Figure 7. Tafel plots of steel specimens: (a) uncoated; coated with: (b) modified TiO₂, (c) pure methylhydro-silicone oil, (d) fluoro-methylhydro-silicone oil, (e) TiO₂/fluoro-methylhydro-silicone oil in 3.5% NaCl solution

Table 1. Corrosion potentials and corrosion current densities of different samples

Coating	Corrosion potential/V	corrosion current density(A/cm ²)	β_a (V/dec)	β_c (V/dec)
Bare steel substrate	-1.15	7.68×10^{-3}	0.07	0.13
Nano modified TiO ₂ methylhydro-silicone oil	-0.91	1.67×10^{-4}	0.09	0.14
fluoro-methylhydro-silicone oil	-0.98	1.57×10^{-4}	0.12	0.13
TiO ₂ /fluoro-methylhydro-silicone oil	-0.93	9.82×10^{-5}	0.11	0.14
	-0.85	3.44×10^{-5}	0.16	0.16

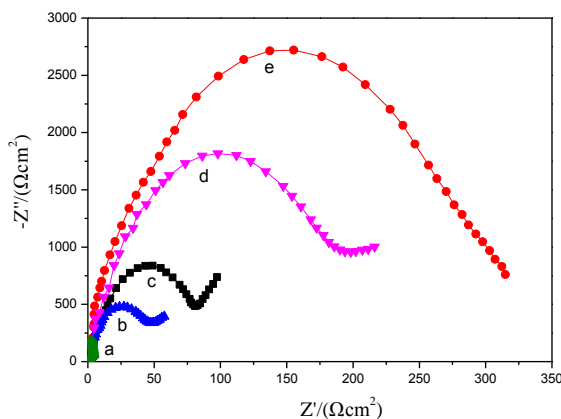


Figure 8. EIS curves of steel specimens:(a) uncoated; coated with: (b) modified TiO₂, (c) pure methylhydro-silicone oil, (d) fluoro-methylhydro-silicone oil, (e) TiO₂-fluoro-methylhydro-silicone oil in 3.5% NaCl solution

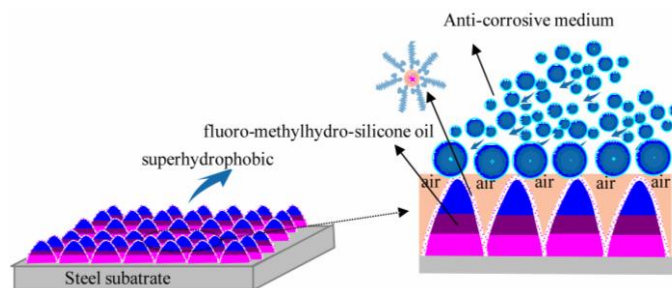


Figure 9. Anti-corrosive mechanism of TiO₂/ organic composite coating

4. CONCLUSION

In this paper, we fabricated TiO₂/fluoro-methylhydro-silicone oil composite coating with abundant surface microstructures via a simple method by using nano-TiO₂ particle and methylhydro-silicone oil as raw materials. The hydrophobicity and surface structure of the composite coating were described by thermo gravimetric analysis, Scanning electron microscopy, Fourier transform infrared and Contact angle analyzer. The results showed the final composite coating exhibits superhydrophobic performance with a static contact angle of $151.5 \pm 1^\circ$ and a rolling angle of 6° . The corrosion of the hybrid coating was characterized by electrochemical methods, such as polarization curve measurement and Electrochemical impedance measurements. The results indicated that the TiO₂/fluoro-methylhydro-silicone oil composite coating both had good hydrophobicity and anti-corrosion performance.

References

1. A. M. Escobar, N. Llorca-Isern. *Applied Surface Science*, 305 (2014) 774-782.
2. K. Yanagisawa, M. Sakai, T. Isobe, S. Matsushita, A. Nakajima. *Applied Surface Science*, 315 (2014) 212-221.
3. F J Wang, T H Shen, C Q Li, W Li, G L Yan. *Applied Surface Science*, 317 (2014) 1107-1112.
4. S Q He, J Q Wei, H F Wang, D S Sun, Z H Yao, C S Fu, R Q Xu, Y Jia, H W Zhu, K L Wang, D H. Wu. *Nanoscale Research Letters*, 8 (2014) 412-417.
5. W Lei, Z H Jia, J C He, T M Cai. *Applied Thermal Engineering*, 62 (2014) 507-512.
6. J Li, Z J Jing, Y X Yang, Q T Wang, Z Q Lei. *Surface & Coatings Technology*, 258 (2014) 973-978.
7. J Li , X H Liu , Y P Ye, H D Zhou, J M Chen. *Colloids and Surfaces A: Physicochemical and Engineering Aspects*, 384 (2011)109-114.
8. Shi Xiaofeng F, Lu Shixia, Xu Wenguo. *Materials Chemistry and Physics*, 134 (2012) 657-663.
9. M. Ramezani, M. R. Vaezi, A. Kazemzadeh. *Applied Surface Science*, 317 (2014) 147-153.
10. Y Liu, J D Liu, S Y Li, Y M Wang, Z W Han, L Q Ren. *Colloids and Surfaces A: Physicochem. Eng. Aspects*, 466 (2015) 125-131.
11. B Xu, J Ding, L Feng, Y Y Ding, F Y Ge, Z S Cai. *Surface & Coatings Technology*, 262 (2015) 70-76.
12. J.D. Brassard, D.K. Sarkar, J. Perron, A. Audibert-Hayet, D. Melot. *Journal of Colloid and Interface Science*, 11 (2014) 76-82.

13. N Wang, D S Xiong. *Applied Surface Science*, 305 (2014) 603-608.
14. X Zhang, Y G Guo, Z J Zhang, P Y Zhang. *Applied Surface Science*, 284 (2013) 319-323.
15. Y Liu, S Y Li, J J Zhang, Y M Wang, Z W Han, L Q Ren. *Chemical Engineering*, 262 (2015) 70-76.
16. H Li, C Y Huang, L Zhang, W Q Lou. *Applied Surface Science*, 467 (2015) 224-232.
17. Z Q Dong, X H Ma, Z L Xu, W T You, F B Li. *Desalination*, 347 (2014) 175-183.
18. D L Zang, F Liu, M Zhang, X G Niu, Z X Gao, C Y Wang. *Chemical Engineering Journal*, 262 (2015) 210-216.
19. J Liang, Y C Hu, Y Q Wu, H Chen. *Surface & Coatings Technology*, 240 (2014) 145-153.
20. Z Yu, W Song, L Chen, Y. Park, B Zhao, Q Cong. *Colloids and Surfaces A: Physicochem. Eng. Aspects*, 467 (2015) 224-232.
21. L T Yin, J Yang, Y C Tang, L Chen, H Tang, C S Li. *Applied Surface Science*, 316 (2014) 259-263.
22. W W Zhang, P Lu, L Y Qian, H N Xiao. *Chemical Engineering Journal*, 250 (2014) 431-436.
23. Z W Wang, Q Li, Z X She, F N Chen, L Q Li, X X Zhang, P Zhang. *Applied Surface Science*, 271 (2013) 182-192.
24. R M Wu, G H Chao, H Y Jiang, Y Hu, A Q Pan. *Material Letters*, 142 (2015) 176-179.
25. Y F Wang, B X Li, T X Liu, C Y Xu, Z W Ge. *Colloids and Surfaces A: physicochem. Eng.Aspects*, 441 (2014) 298-305.
26. P P Li, X H Chen, G B Yang, L G Yu, P Y Zhang. *Applied Surface Science*, 300 (2014) 184-190.
27. Annaso B. Gurav, Q F Xu, Sanjay S. Latthe, R.S. Vhatkar, S H Liu, Hyun Yoon, Sam S. Yoon. *ScienceDirect Ceramics International*, 41 (2015) 3017-3023.
28. K. Nakano, S. Akita, M. Yamanaka. *Colloid Polymer Science*, 292 (2014) 1475-1478.
29. A. Siddaramanna, N. Saleema, D.K. Sarkar. *Applied Surface Science*, 311 (2014) 182-188.
30. J Z Ma, Y H Liu, Y Bao, J L Liu, J Zhang. *Advances in Colloid and Interface Science*, 197-198 (2013)118-131.
31. Y W Hu, S Y Huang, S Liu, W Pan. *Applied Surface Science*, 258 (2012) 7460-7464.
32. R. Ramanathan, D. E. Weibel. *Applied Surface Science*, 258 (2012) 7950-7955.
33. Y F Wang, B X Li, T X Liu, C Y Xu, Z W Ge. *Colloids and Surface A: Physicochemical and Engineering Aspects*, 441 (2014) 298-305.
34. A. Safaee, D. K. Sarkar, M. Farzaneh. *Applied Surface Science*, 254 (2008) 2493-3498.
35. Y S Zheng, Y He, Y Q Qing, Z H Zhuo, Q Mo. *Applied Surface Science*, 258 (2012) 9859-63.
36. J. MacMullen, Z Y Zhang, J. Radulovic, C. Herodotou, M. Totomis, H. N. Dhakal, N. Bennett. *Energy and Buildings*, 52 (2012) 86-92.
37. X M Shi, T. A. Nguyen, Z Y Suo, J L Wu, J Gong, R. Avci. *Surface & Coating Technology*, 206 (2012) 3700-3713.
38. D. S. Kim, B. K. Lee, J. Yeo, M. J. Choi, W. Yang, T. H. Kwon. *Microelectronic Engineering*, 86 (2009) 1375-1378.
39. B. Bhushan, Y. C. Jung. *Progress in Materials Science*, 56 (2011) 1-108.
40. I. Yilgor, S. Bilgin, M. Isik, E. Yilgor. *Polymer*, 53 (2012) 1180-1188.
41. W Y Liu, Y T Luo, L Y Sun, R M Wu, H Y Jiang, Y J Liu. *Applied Surface Science*, 264 (2013) 872-878.
42. T C Wang, L J Chang, B. Hatton, J Kong, G Chen, Y Jia, D S Xiong, C P Wong. *Materials Science and Engineering C*, 43 (2014) 310-316.
43. Z Z Zhang, X T Zhu, J Yang. *Materials Science & Processing Applied Physics A*, 108 (2012) 601-606.
44. H. Hammache, L. Makhloufi, B. Saidani. *Corrosion Science*, 45 (2003) 2031-2042.
45. J. R. Santos Jr., L. H. Mattoso, A. J. Matheo, *Electrochimica Acta*, 43 (3-4) (1998) 309.
46. M. Merisalu, T. Kahro, J. Kozlova, A. Niilisk, A. Nikolajev, M. Marandi, A. Floren, H. Alles, V. Sammelselg. *Synthetic Metals*, 200 (2015) 16-23.

47. B.H. Kim, K. S. Yang, H.G. Woo, K. Oshida. *Synthetic Metals*, 161 (2011) 1211-1216.
48. Y Q Qing, C N Yang, Y Shang, Y Z Sun, C S Liu. *Colloid and Polymer Science*, 293 (2015) 1809-1816.
49. C B Hu, Y S Zheng, Y Q Qing, F L Wang, C Y Mo, Q Mo. *Journal of Inorganic and Organometallic Polymer and Materials*, 25 (2015) 583-592.

© 2015 The Authors. Published by ESG (www.electrochemsci.org). This article is an open access article distributed under the terms and conditions of the Creative Commons Attribution license (<http://creativecommons.org/licenses/by/4.0/>).

© 2015 The Authors. Published by ESG (www.electrochemsci.org). This article is an open access article distributed under the terms and conditions of the Creative Commons Attribution license (<http://creativecommons.org/licenses/by/4.0/>).